Photochemistry of Highly Alkylated Dienes: Computational Evidence for a Concerted Formation of Bicyclobutane

Marco Garavelli,† Barbara Frabboni,† Monica Fato,† Paolo Celani,‡ Fernando Bernardi,† Michael A. Robb,*,‡ and Massimo Olivucci*,†,§

Contribution from the Dipartimento di Chimica "G. Ciamician", Universitá di Bologna, via Selmi n. 2, Bologna I-40126, Italy, and Department of Chemistry, King's College, London Strand, London WC2R 2LS, United Kingdom

Received August 10, 1998. Revised Manuscript Received November 19, 1998

Abstract: In this report, high-level ab initio quantum chemical computations (MC−SCF and multireference Møller−Plesset perturbation theory) are used to compute the composite $S_2 \rightarrow S_1 \rightarrow S_0$ relaxation/reaction paths describing the photorearrangement of the highly alkylated diene 2,3-di-*tert*-butylbuta-1,3-diene (**1**) and of the parent compound *s-cis*-buta-1,3-diene. Reaction path computations require, typically, hundreds of energy and gradient evaluations. For this reason, we have defined, validated, and employed a simple *hybrid* method designed to simulate a *tert*-butyl group at the computational cost of a methyl group. Despite the fact that the method only treats specific substituents (e.g. *tert*-butyl groups) embedded in a specific environment (e.g. a hydrocarbon skeleton) we show that it can be successfully employed in mechanistic studies where steric factors dominate. The analysis of the computed relaxation coordinate provides a mechanistic explanation for the different strained photoproducts generated by photolysis of the parent and substituted dienes. In particular, we show that while *s-cis*-buta-1,3-diene produces cyclobut-1-ene via a disrotatory ring-closure path, the two bulky *tert*-butyl substituents in **1** greatly enhance the production of a highly strained bicyclo[1.1.0]butane derivative (which forms only in traces when the parent compound is photolyzed) by driving the excited-state relaxation along a concerted and synchronous path characterized by a conrotatory rotation of the two terminal methylenes.

1. Introduction

The photolysis of highly alkylated dienes often leads to production of strained products which are either undetected or produced in traces when the parent compound is photolyzed. For example, in recent experimental work on 2,3-di-*tert*-butylbuta-1,3-diene (**1**), Hopf et al.[1] have shown that direct irradiation (450 W Hg high-pressure lamp) of **1** in dilute solution

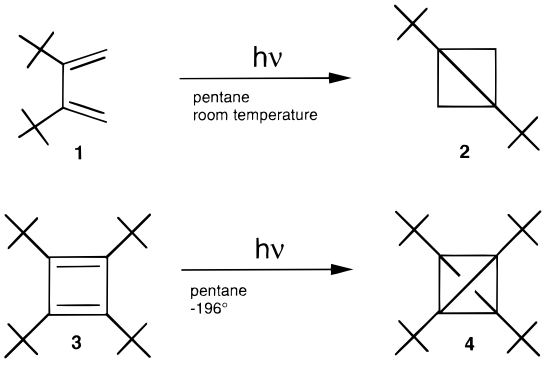

leads to production of 1,2-di-*tert*-butylbicyclo[1.1.0]butane (**2**) as the only photoproduct (60% yield after 60 min irradiation). In contrast, the photolysis of the parent compound buta-1,3-diene yields cyclobut-1-ene as the major photoproduct[2] and the bicyclo[1.1.0]butane (indicated as bicyclobutane from now on) is only present in traces. An even more spectacular example is the photolysis of 1,2,3-tri- or 1,2,3,4-tetra-*tert*-butylcyclobuta-1,3-diene (**3**), which produces a derivative (**4**) of the smallest possible polyhedral hydrocarbon: tetrahedrane. However, the tetrahedrane does not form when a less substituted reactant is photolyzed.[3]

In these examples, the different photoreactivity of the substituted versus the parent compounds is attributed to the high strain induced by two or more bulky *tert*-butyl groups located in adjacent positions. Indeed, this fact is supported by the X-ray structural analysis[4] and electron diffraction data[5] of **1**: the equilibrium conformation of the butadiene moiety is 82−84° twisted about its single bond. It is clear that the substituents will affect the equilibrium conformation or, in the case of compound **3**, the ring strain. However, it is not clear how the steric repulsions and large masses can control the outcome of the photoreaction, i.e., whether they affect the transient excited-state structure and its evolution, the mechanism of decay, or the cooling of a hot ground-state intermediate.

tert-Butyl groups are rather versatile substituents. Hopf et al. have recently introduced new synthetic techniques which allow bulky alkyl groups (like *tert*-butyl and isopropyl) to be inserted in dienes and longer polyene chains.[6] In this way

† Universitá di Bologna.

‡ King's College.

§ Present address: Istituto di Chimica Organica, Università degli Studi di Siena, Pian dei Mantellini 44, I-53100 Siena, Italy. E-mail: olivucci@unisi.it.

(1) Hopf, H.; Lipka, H.; Traettemberg M. *Angew. Chem., Int. Ed. Engl.* **1994**, *33*, 204−205.

(2) (a) Srinivisan, R. *J. Am. Chem. Soc.* **1963**, *85*, 4045−4046. (b) Leigh, W. J. *Can. J. Chem.* **1993**, *71*, 147.

(3) Maier, G. *Angew. Chem., Int. Ed. Engl.* **1988**, *27*, 309−335.

(4) Roth, W. R.; Adamczak, O.; Breuckmann, R.; Lennartz, H.-W.; Boese, R. *Chem. Ber.* **1991**, *124*, 2499−2521.

(5) Traettemberg, M.; Hopf, H.; Lipka, H. Unpublished results.

(6) Hopf, H.; Lipka, H. *Chem. Ber.* **1991**, *124*, 2075−2084.

10.1021/ja982864e CCC: $18.00
Published on Web 02/05/1999

polyalkylated polyenes with different degree of substitution and distribution of the substituents can be designed. This type of chemistry offers the opportunity for the rational design of strained compounds and other new materials. Indeed, in the past *tert*-butyl groups have been used to control the reactant equilibrium conformation in hexatriene photochemistry and for related mechanistic studies.[7] Compounds of limited complexity like **1** and **3** can be regarded as prototype systems which can be used for investigating the effect of strategically placed bulky groups. In this paper we present a computational investigation of the photorearrangement mechanism of **1**.

The rational design of strained photoproducts requires a detailed knowledge of the way in which bulky groups control the excited- and ground-state evolution of the reactant skeleton. During the past few years significant progress in the computation of the excited states of isolated molecules has been achieved. The excited-state energetics of sizable polyenes (from butadiene to octatetraene) can be computed with reasonable accuracy using high-level ab initio quantum chemical methodologies,[8] and the reaction coordinates, evaluated by computing the minimum energy paths (MEP) for isomerization and rearrangement of polyenes, do rationalize the available experimental data.[9] Thus, one has some confidence that such methods can be used to study the basic features determining the formation of **2** via photolysis of compound **1**.

In this report, high-level ab initio quantum chemical computations (MC−SCF[10a] and multireference Møller−Plesset perturbation theory[11a]) are used to investigate the MEP describing the excited-state relaxation of **1** and of the corresponding parent compound *s-cis*-buta-1,3-diene (indicated as *cis*-butadiene in the rest of the paper). This MEP has three sequential branches which span the S_2, S_1, and S_0 potential energy surface, respectively. For the parent compound, we have documented[12] two distinct energy surface crossings (i.e. the S_2/S_1 and S_1/S_0 conical intersections[13]) that connect the S_2 to the S_1 path and the S_1 to S_0 path, respectively. Each path provides information on the force field that the molecule "feels" on each state and that, ultimately, determines the molecular motion. In addition, the molecular geometry of the system at S_2/S_1 and S_1/S_0 crossings provides information on the geometrical deformation required to induce radiationless deactivation to the lower state. While the relaxation process could be modeled by means of quantum or semiclassical dynamics, the system under investigation is still too large for a systematic investigation of this type. Thus in this paper *we shall focus on the structure of the energy surfaces which control the relaxation and isomerization processes*.

High-level ab initio quantum chemical computations of the type used in this paper are very expensive. Typically, the increase in CPU time of ab initio post-SCF computations (such as the MC−SCF method used here) scales as N^4 (where N is the number of basis functions used in the computations). Since a computational investigation, such as that outlined above, usually requires hundreds of energy and gradient evaluations, each *tert*-butyl group attached to the parent's framework increases the computational cost substantially. For this reason, and looking forward to applications to larger systems containing more than two bulky substituents, we have implemented a new *hybrid* methodology designed to simulate a *tert*-butyl group at the computational cost of a methyl group. In this method the *tert*-butyl groups of **1** are *not* treated at the MC−SCF level. Rather they are replaced by methyl groups and the steric effect of *tert*-butyls is simulated by applying suitable parametrized pair potentials to the methyl groups. We shall demonstrate that such hybrid methodology can be useful when one is interested in the mechanistic aspects of the presence of bulky substituents which are not directly involved in the bond-breaking−bond-forming process.

After absorption of a photon a diene is promoted to its spectroscopic state (a symmetry-allowed $\pi-\pi^*$ singly excited state) S_2. As mentioned above, it has been shown[12] that, for *cis*-butadiene, this event initiates a relaxation process leading to a lower lying dark state (i.e. symmetry-forbidden $\pi-\pi^*$ doubly excited state) S_1 and finally to the ground state (S_0) by decay through two sequential radiationless decay channels. In what follows, we shall show that photoexcitation of the highly alkylated diene **1** and of the parent compound results in two different transient excited-state species with C_2 and C_s symmetries, respectively. Most importantly, the computed *three-state* ($S_2 \rightarrow S_1 \rightarrow S_0$) relaxation paths describing the excited- and ground-state evolution of these species span structurally different regions of the three potential energy surfaces. In particular, the S_1 relaxation paths, which connect the S_2/S_1 and S_1/S_0 intersections (i.e. the decay channels), develop entirely along a (C_2) *totally symmetric* coordinate in **1** but involve a *fully asymmetric* out-of-plane distortion in *cis*-butadiene. Furthermore, the molecular structure of the S_1/S_0 intersection and the structure of the accessible S_0 relaxation paths indicate that the highly strained bicyclobutane **2** can be formed in a *concerted* and *synchronous* fashion from **1** but that cyclobut-1-ene must be the favored strained photoproducts of *cis*-butadiene photolysis.

2. Computational Methods

(i) Ab Initio Quantum Chemical Computations. All MC−SCF energy, gradient, and frequency computations have been carried out using a complete active space (CAS) with the double-ζ + polarization (6-31G*) basis sets available in Gaussian 94.[10b] The S_2, S_1, and S_0 minima, transition states, and MEPs have been computed using a 4 electrons in 4 orbitals CAS. The S_2 MEP of compound **1** has been computed imposing C_2 symmetry in order to avoid convergence failure. However, to confirm that the S_2 C_2 minimum is an energy minimum with respect to the full space of the internal coordinates, it has been reoptimized at the CIS level of theory to test the stability of this

(7) (a) Jacobs, H. J. C.; Cornelisse, J. *Pure Appl. Chem.* **1995**, *67*, 63−70. (b) Jacobs, H. J. C.; Cornelisse, J.; Brouwer *Photochem. Photobiol. A: Chem.* **1988**, *42*, 117 (c) *Ibid.* **1988**, *42*, 313.

(8) (a) Serrano-Andrés, L.; Merchán, M.; Nebot-Gil, I.; Lindh, R.; Roos, B. O. *J. Chem. Phys.* **1993**, *97*, 9360−9368. (b) Serrano-Andrés, L.; R.; Roos, B. O.; Merchán, M. *Theor. Chim. Acta* **1994**, *87*, 387−402. (c) Serrano-Andrés, L.; Lindh, R.; Roos, B. O.; Merchán, M. *J. Phys. Chem.* **1993**, *97*, 9360−9368.

(9) Celani, P.; Garavelli, M.; Ottani, S.; Bernardi, F.; Robb, M. A.; Olivucci, M. *J. Am. Chem. Soc.* **1995**, *117*, 11584−11585.

(10) (a) Roos, B. O. *Adv. Chem. Phys.* **1987**, *69*, 399−446. (b) The MC−SCF program we used is implemented in the following: Frisch, M. J.; Trucks, G. W.; Schlegel, H. B.; Gill, P. M. W.; Johnson, B. G.; Robb, M. A.; Cheeseman, J. R.; Keith, T.; Petersson, G. A.; Montgomery, J. A.; Raghavachari, K.; Al-Laham, M. A.; Zakrzewski, V. G.; Ortiz, J. V.; Foresman, J. B.; Peng, C. Y.; Ayala, P. Y.; Chen, W.; Wong, M. W.; Andres, J. L.; Replogle, E. S.; Gomperts, R.; Martin, R. L.; Fox, D. J.; Binkley, J. S.; Defrees, D. J.; Baker, J.; Stewart, J. P.; Head-Gordon, M.; Gonzalez, C.; Pople, J. A. *Gaussian 94*, revision B.2; Gaussian, Inc.: Pittsburgh, PA, 1995.

(11) (a) Andersson, K.; Malmqvist, P.-A.; Ross B. O. *J. Chem. Phys.* **1992**, *96*, 1218. (b) Andersson, K.; Blomberg, M. R. A.; Fülscher, M.; Kellö, V.; Lindh, R.; Malmqvist, P.-A.; Noga, J.; Olsen, J.; Roos, B. O.; Sadlej, A. J.; Siegbahn, P. E. M.; Urban, M.; Widmark, P. O. *MOLCAS*, version 3; University of Lund: Lund, Sweden 1994.

(12) (a) Celani, P.; Bernardi, F.; Olivucci, M.; Robb, M. A. *J. Chem. Phys.* **1995**, *102*, 5733. (b) Olivucci, M.; Ragazos, I. N.; Bernardi, F.; Robb, M. A. *J. Am. Chem. Soc.* **1992**, *114*, 8211. (c) Olivucci, M.; Bernardi, F.; Ottani, S.; Robb, M. A. *J. Am. Chem. Soc.* **1994**, *116*, 2034.

(13) (a) Bernardi, F.; Olivucci, M.; Robb, M. A. *Chem. Soc. Rev.* **1996**, *25*, 321−328. (b) Bernardi, F.; Olivucci, M.; Michl, J.; Robb, M. A. *Spectrum* **1996**, *9*, 1−6.

Scheme 1

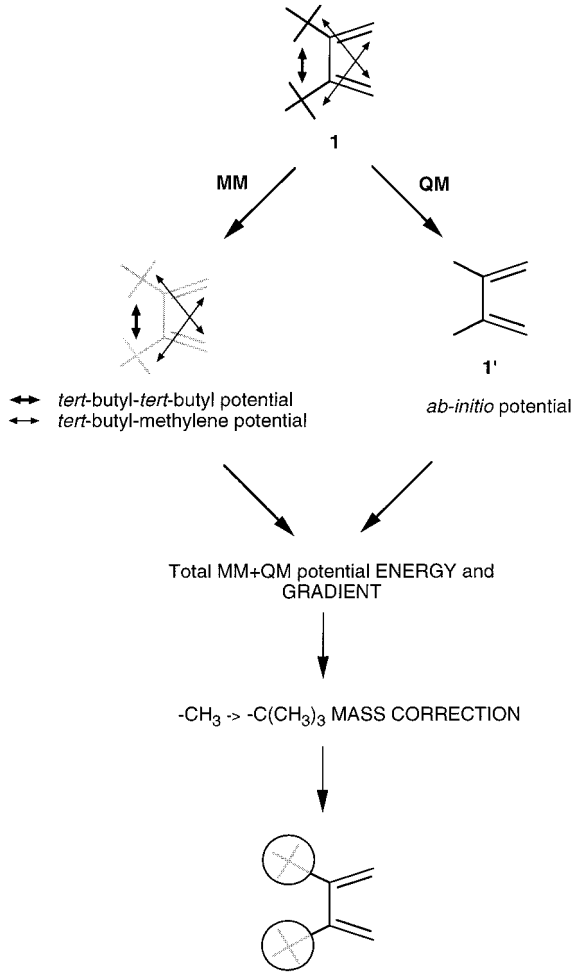

stationary point with respect to non-totally-symmetric deformations. To improve the energetics by including the effect of dynamic electron correlation, the energies have been recomputed using multireference Møller−Plesset perturbation theory method PT2F[11a] included in MOLCAS-3.[11b] For all states the MC−SCF zeroth order wave function used for the PT2F computation has been improved by using the standard double-ζ + polarization + diffuse (6-31+G*) basis set.

(ii) Simulation of the *tert*-Butyl Substituents. As mentioned in the Introduction, we have implemented a simple QM−MM hybrid methodology for computing the S_2, S_1, and S_0 potential energy surfaces of polyalkylated dienes. The method is similar, in spirit, to the "two layers" IMOMM method proposed by Morokuma et al.[14] However, it is less "flexible" since it is based on the parametrization of the interaction of specific groups (i.e. *tert*-butyl groups) embedded in a specific environment (i.e. a hydrocarbon skeleton). The "flow chart" which defines the method is given in Scheme 1 for the case of compound **1**.

The interactions between the substituents and between the substituents and the environment are simulated by specially designed MM-type pair potentials. Thus the potential energy and gradient of **1** are given by the sum of quantum mechanical (QM) and purely mechanical (MM) contributions. The QM contribution is computed at the ab initio MCSCF level of theory on a structure where the computationally expensive *tert*-butyl groups are replaced by the smaller methyl groups (compound **1′**). At the same time the MM steric interactions in **1** (see double arrows in Scheme 1) between the original *tert*-butyl (*tert*-butyl−*tert*-butyl) and between the *tert*-butyl and the methylene groups (*tert*-butyl−methylene) are modeled via inexpensive parametrized analytic potentials. The total energy and gradient for the state of interest (i.e. either S_2, S_1, or S_0) is then evaluated by adding the *tert*-butyl steric energy and gradient to the ab initio energy and gradient of the corresponding **1′**. The resulting values can be used for carrying out geometry optimization using the available standard methodology. In the case of MEP and IRD computations (see subsection iii below) one also needs to correct the masses of the methyl substituents in compound **1′**. This is done by augmenting the masses of each hydrogen atom in the two methyl substituents to that of a $-CH_3$ group.

(14) (a) Froese, R. D. J.; Musaev, D. G.; Morokuma, K. *J. Am. Chem. Soc.* **1998**, *120*, 1581−1587. (b) Maseras, F.; Morokuma, K. *J. Comput. Chem.* **1995**, *16*, 1170.

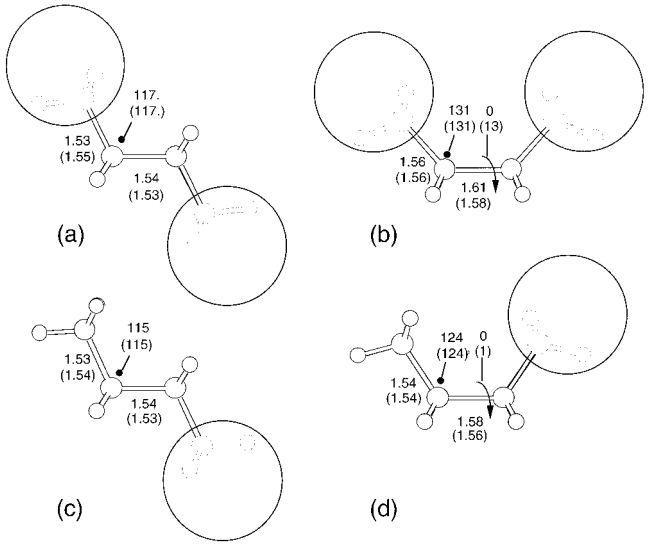

Figure 1. Hybrid and ab initio optimized structures (the relevant geometrical parameters given in Å and deg) for (a) 1,2-di-*tert*-butylethane MIN, (b) 1,2-di-*tert*-butylethane TS, (c) 1-*tert*-butylpropane MIN, and (d) 1-*tert*-butylpropane TS. The values in parentheses refer to the ab initio RHF/6-31G* structure.

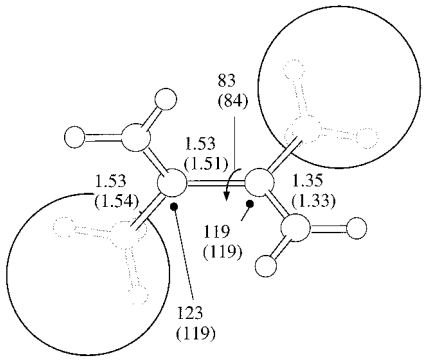

Figure 2. Optimized structure of compound **1** (the relevant geometrical parameters given in Å and deg). The values in parentheses refer to the molecular geometry determined via X-ray structural analysis.

While the flow chart (Scheme 1) of our hybrid method shows that it is simple, the parametrization process, which yields good functional forms and parameters for the two MM steric potentials, is more complex, and the evaluation of such potentials is based upon the parametrization of the conformational structure of the S_0 energy surface of three different molecules: *n*-butane, 1-*tert*-butylpropane, and 1,2-di-*tert*-butylethane. The details of the parametrization procedure, which requires the computation (at the ab initio RHF/6-31G* level) of several energy surface cross-sections, are given in the Appendix.

The accuracy of the method has been tested in two ways: (a) The method has been used to reproduce the ab initio RHF/6-31G* geometry and energetics of the conformational minima and transition states of the 1-*tert*-butylpropane and 1,2-di-*tert*-butylethane (see Figure 1). (b) We have compared the X-ray structural parameters[4] of compound **1** with the equilibrium (gas-phase) molecular structure of **1** determined via geometry optimization using the hybrid method described above. As shown in Figure 2 these two structures are remarkably close. In particular, the essentially identical value for the torsional parameter demonstrates that the balance between the repulsion *tert*-butyl−*tert*-butyl and *tert*-butyl−methylene is correctly reproduced.

Table 1. Multireference Perturbation Theory (PT2F) Absolute (E) and Relative (ΔE) Energies, Where in the Case of 2,3-Di-*tert*-butylbutadiene the Values in Italic Have Been Corrected by the Hybrid Method Defined in the Text and for *cis*-Butadiene the Methodological Details Are in Ref 12a

cis-butadiene[a]				2,3-di-*tert*-butylbutadiene			
structure	state	E (au)[c]	ΔE (kcal mol^{-1})	structure	state	E (au)[c]	ΔE (kcal mol^{-1})
C_{2v}-MIN	S_0		0.0	**C_2-GS**	S_0	−233.7653 (0.80)	
						−233.75537	0.0
	S_1	−155.2678 (0.85)	140.7		S_1	−233.4685[d]	
						−233.4586	186.2
	S_2	−155.2869 (0.85)	128.7[b]		S_2	−233.5221 (0.76)	
						−233.5122	152.6
C_S-ION	S_1	−155.3054 (0.84)	117.1	**C_2-ION**	S_1	−233.5683 (0.75)	
						−233.5510	128.2
	S_2	−155.3070 (0.84)	116.1		S_2	−233.5833 (0.74)	
						−233.5661	118.8
C_S-MIN	S_1	−155.3279 (0.83)	103.0	**S_2/S_1 CI**	S_1	−233.5684 (0.78)	
						−233.5550	125.8
C_S/CI-TS	S_1	−155.3291 (0.84)	102.3		S_2	−233.5659 (0.74)	
S_1/S_0 CI	S_1	−155.3397 (0.84)	95.6			*−233.5524*	127.4
				S_1/S_0 CI	S_0	−233.6150 (0.79)	
						−233.6038	95.1
					S_1	−233.5932 (0.78)	
						−233.5821	108.7
				S_1/S_0 CI (OPT)	S_0	−233.6050 (0.78)	
						−233.5978	98.9
					S_1	−233.5947 (0.78)	
						−233.5875	105.3
					S_2	-233.5083 (0.74)	
						−233.5011	159.6
				C_2-ION (CIS)	S_0	−233.7323 (0.80)	26.0
						−233.7140	
					S_1	−233.5662 (0.76)	130.2
						−233.5478	
					S_2	−233.5897 (0.76)	115.5
						−233.5713	
				C_2-ION (TS)	S_0	−233.7364 (0.80	16.8
						−233.7287	
					S_2	−233.5518 (0.73)	132.6
						−233.5441	

[a] From ref 12a. [b] This *cis*-butadiene ΔE value is from ref 8b. The other ΔE values are computed by adding the corresponding energy difference to this value. [c] In parentheses we give the weight of the MC−SCF reference function (i.e. the zeroth order function) in the first-order function. [d] Estimated CAS-PT2 value.

(iii) Relaxation Path Computation. The composite $S_2 \rightarrow S_1 \rightarrow S_0$ relaxation path for compound **1** is computed in *four* steps. (a) In the first step we compute the energy minima and transition states located on the potential energy surface of the spectroscopic state S_2. (b) In the second step we have explored the structure of the low-lying part of the S_1 energy surface of **1**. We have not been able to locate an equilibrium stationary point on this potential energy surface. Thus we have used the methodology for conical intersection optimization[15] available in Gaussian94[10b] to locate the lowest-lying S_1/S_0 conical intersection point. (c) In the third step, we compute the path describing the S_1 relaxation processes. This has been achieved by first locating the S_2/S_1 intersection point (i.e. the $S_2 \rightarrow S_1$ decay channel). The conical intersection optimization method mentioned in point b cannot be applied to this purpose since the energy gap of the S_2 and S_1 states is overestimated at the MCSCF level of theory (this is due to the very different electronic nature of the two states: ionic for the S_2 and covalent for S_1) and one must apply the PT2F correction to obtain a reliable energy gap. To overcome this difficulty, we have located the crossing point by computing the S_2 and S_1 PT2F energies along a series of points connecting the optimized S_2 minimum to the optimized S_1/S_0 conical intersection. This yields an S_2/S_1 surface crossing point with a totally symmetric molecular structure which is located above the optimized S_2 minimum. Due to the approximate nature of the chosen S_2 reaction coordinate, the resulting value of the crossing relative energy is expected to be an upper limit. The S_2/S_1 surface crossing has then been taken as starting point for the computation of the MEP describing the S_1 relaxation. This MEP has been determined by using a method[16] which locates the initial direction of relaxation (IRD) from the starting point. An IRD corresponds to a local *steepest descent direction*, in *mass-weighted Cartesians*, from a given starting point. (The details of the method used can be found in ref 16a.) Once one or more IRDs have been determined, the associated MEP is computed as *the steepest descent line in mass-weighted Cartesians* using the IRD vector to define the initial direction to follow. (d) Finally, in the fourth and last step, we compute the S_0 MEPs, describing the relaxation and photoproduct formation processes from the S_1/S_0 conical intersection (i.e. the $S_1 \rightarrow S_0$ decay channel). Again, these are computed using the IRD technique discussed above.

3. Results and Discussion

The energy values for all stationary points found on the S_2, S_1, and S_0 potential energy surfaces are reported in Table 1. The resulting composite $S_2 \rightarrow S_1 \rightarrow S_0$ relaxation path is represented by bold lines in Figure 3 on the three potential energy sheets S_2, S_1, and S_0. Equilibrium stationary points are represented by full circles, transition states by open squares, and intersection points (**S_2/S_1 CI** and **S_1/S_0 CI**) by open circles. The energy profiles along the S_2 paths (path **I** in Figure 3a,b)

(15) Bearpark, M. J.; Robb, M. A.; Schlegel, H. B. *Chem. Phys. Lett.* **1994**, *223*, 269−274.

(16) (a) Celani, P.; Robb, M. A.; Garavelli, M.; Bernardi, F.; Olivucci, M. *Chem. Phys. Lett.* **1995**, *243*, 1−8. (b) Garavelli, M.; Celani, P.; Fato, M.; Bearpark, M. J.; Smith, B. R.; Olivucci, M.; Robb, M. A. *J. Phys. Chem.* **1997**, *101*, 2023−2032.

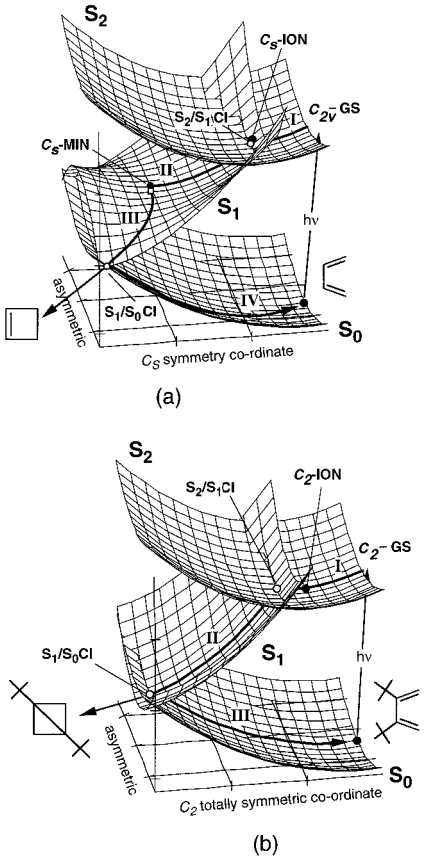

Figure 3. Three-dimensional representation of the S_0, S_1, and S_2 potential energy surfaces of (a) *cis*-butadiene and (b) compound **1**. The bold lines correspond to the computed relaxation/reaction paths (paths **I**−**IV**) discussed in the text. The symbols (open circle, full circle, and open square) and labels indicate the relevant stationary and crossing points located on the three energy sheets. Notice that, in the case of *cis*-butadiene, there are two paths on the S_1 sheet: path **II** (full line) which describes the S_1 relaxation process along a totally symmetric (C_s) coordinate and path **III** (light line) which describes nonadiabatic isomerization along an asymmetric coordinate. However, on the S_1 sheet of compound **1** this asymmetric path does not exist.

end at two S_2 minima (***C*$_s$-ION** and ***C*$_2$-ION**) located near two S_2/S_1 crossing points. From these points begins an S_1 relaxation path. In *cis*-butadiene this path spans two domains. The first domain (**II** in Figure 3a) corresponds to a valley centered along a C_s symmetric coordinate connecting the S_2/S_1 crossing point to an S_1 stationary point. The second domain (**III** in Figure 3a) is defined by a fully asymmetric coordinate which connects the stationary point to the S_1/S_0 crossing region through a substantially barrierless path (the transition structure corresponding to the open square in Figure 3a and connecting ***C*$_s$-MIN** to the S_1/S_0 crossing disappears when a high level of theory is used. See also the discussion in subsection i below). This coordinate is dominated by torsional deformations, and it is therefore *orthogonal* to the coordinate describing the initial relaxation. In deep contrast the S_1 relaxation path of compound **1** spans a single totally symmetric (C_2) domain (path **II** in Figure 3b) which connects the S_2/S_1 and the S_1/S_0 crossing regions. Finally, the S_0 path (**IV** in Figure 3a and **III** in Figure 3b) connects the S_1/S_0 crossing to the reactant potential energy well through a very steep and barrierless valley.

It is clear from Figure 3 that the depopulation of S_2, i.e., depletion of the ***C*$_s$-ION** and ***C*$_2$-ION** transients initiates a relaxation process which starts in the region of the S_2/S_1 crossings. In the following subsections we describe the details of the relaxation paths summarized above. In particular, in subsection i we deal with the S_2 decay and subsequent relaxation on the S_1 potential energy surface and in subsection ii we describe the relaxation and isomerization path on S_0.

(i) Depopulation of the Spectroscopic State and Relaxation on S_1. In Figure 4a,b we report the computed MEP along the S_2 and S_1 potential energy surfaces for *cis*-butadiene and compound **1**, respectively. According to this diagram the depopulation of S_2 must be induced by a symmetric displacement toward the S_2/S_1 crossing which involves simultaneous expansion of the double bonds and contraction of the single bonds. Notice that the S_2 relaxation coordinate of *cis*-butadiene has C_s symmetry (i.e. it has a symmetry plane across the central C−C bond) consistent with a disrotatory motion of its two terminal methylenes (as previously discussed,[12a] this is consistent with the prediction of the photochemical orbital symmetry rules[17] for electrocyclization to cyclobut-1-ene). In contrast, compound **1** relaxes along a C_2 totally symmetric coordinate (i.e. it has a 2-fold symmetry axis through the central C−C bond) which corresponds to the photochemically forbidden path in terms of orbital symmetry rules. Thus, this path is imposed by the bulky *tert*-butyl substituents.

While in *cis*-butadiene the crossing is located right at the bottom of the S_2 well, the S_2-S_1 energy gap at the S_2 minima of compound **1** is ca. 9 kcal mol^{-1}. Although, this is not a large gap, it should result in a S_2 lifetime which is much longer than that expected[12a] (and observed[18]) for the parent compound. Further, the estimated S_2 barrier for decay of **1** at the S_2/S_1 crossing, is in the range 7−9 kcal mol^{-1}. However, as mentioned in section 2, this value corresponds to an upper limit. The highly twisted ***C*$_2$-ION** minimum is also connected via a conventional transition state to a different conformer of C_2 symmetry which is about 3.3 kcal mol^{-1} lower in energy (see Table 1). The conformational interconversion is dominated by the change in twisting angle which decreases from 127° in ***C*$_2$-ION** to 11°. Despite the slightly higher stability of this almost planar S_2 conformer we do not regard it as a relevant intermediate of the photoreaction. First, the relaxation from the FC point (***C*$_2$-GS**) leads invariably to ***C*$_2$-ION**, and second, the conformational conversion of ***C*$_2$-ION** is impaired by a barrier more than 5 kcal mol^{-1} larger than the barrier to $S_2 \rightarrow S_1$ decay through the **S_2/S_1 CI** intersection. The structures of the computed ground-state reactant and S_2/S_1 and S_1/S_0 intersection points are given in Figure 5a−c, respectively.

After the $S_2 \rightarrow S_1$ decay the system accelerates along the steep S_1 MEP (path **II** in Figure 4a−b). Along this path the parent and substituted compound both maintain the original C_s and C_2 symmetry. In *cis*-butadiene path **II** ends at a stationary point ***C*$_s$-MIN** where the S_1 and S_0 gap is ca. 60 kcal mol^{-1}. Any further progression in the same direction does not lead to a gap reduction. In contrast, path **II** in compound **1** ends at a S_1/S_0 crossing point (**S_1/S_0 CI**) of C_2 symmetry. This crossing point does not correspond to the lowest lying crossing point on the S_1 energy surface. Rather, minimization of this **S_1/S_0 CI** structure yields a structure (also of C_2 symmetry) which lies ca. 3 kcal mol^{-1} lower in energy. This crossing structure corresponds to the global minimum of the S_1 energy surface.

To confirm the existence of an energy valley driving the relaxation process along path **II**, we have performed a vibrational frequency analysis at a few selected MEP points (see ref

(17) Woodward, R. B.; Hoffmann, R. *Angew. Chem., Int. Ed. Engl.* **1969**, *8*, 781.
(18) (a) Trulson, M. O.; Mathies, R. A. *J. Phys. Chem.* **1990**, *94*, 5741. (b) Vaida, V. *Acc. Chem. Res.* **1986**, *19*, 114−120.

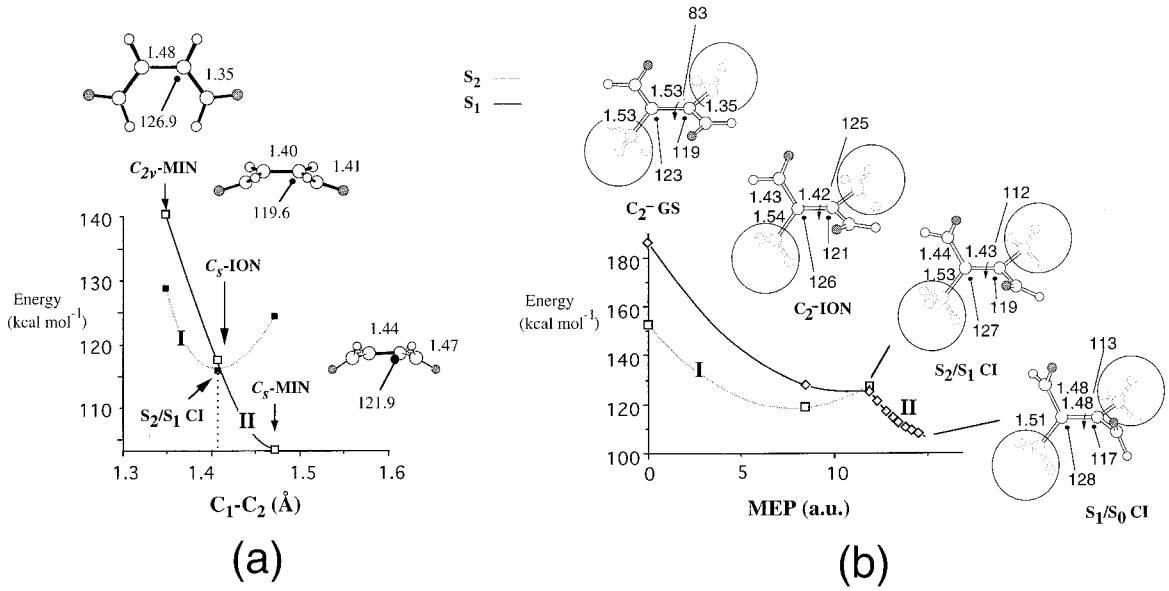

Figure 4. (a) Energy profiles along the two MEPs (paths **I** and **II**) describing the relaxation of *cis*-butadiene from the FC (***C*$_{2v}$-MIN**), S_2/S_1 crossing (***C*$_S$-ION**), and S_1 minimum (***C*$_S$-MIN**) points. Full squares and open squares curves define the S_2 ($1B_2$) and S_1 ($2A_1$) branches of the *excited-state* relaxation path. The energies of all points have been scaled to match the PT2F energies of ***C*$_{2v}$ MIN**, ***C*$_S$-ION**, and ***C*$_S$-MIN** (see Table 1). The structures (geometrical parameters in Å and deg) document the geometrical progression along the relaxation path. (b) Energy profiles along the two MEPs (paths **I** and **II**) describing the relaxation of compound **1** from the FC (***C*$_2$-GS**), S_2 minimum (***C*$_2$-ION**), S_2/S_1 crossing (**S_2/S_1 CI**), and S_1/S_0 crossing (**S_1/S_0 CI**) points. Open squares and open diamonds curves define the S_2 (1B) and S_1 (2A) branches of the *excited-state* relaxation path. The energies of all points have been scaled to match the PT2F energies of ***C*$_2$-GS**, ***C*$_2$-ION**, **S_2/S_1 CI**, and **S_1/S_0 CI** (see Table 1). The structures (geometrical parameters in Å and deg) document the geometrical progression along the relaxation path.

19 for previous work of this type). The vibrational frequencies at nonstationary points (i.e. points with a nonzero energy gradient such as the MEP points) are obtained from the computed Hessian by projection onto the **n** - 1-dimensional space orthogonal to the energy gradient. The diagonalization of this Hessian yields the normal modes and frequencies along the **n** − 1 orthogonal space.[20,21] While a valley is characterized by **n** − 1 *real* frequencies (i.e. the curvature of the energy surface is positive along all **n** − 1 modes) a ridge may have one or more imaginary frequencies. In the case of *cis*-butadiene all frequencies computed at both the 0.5 and 1.5 au distance from the S_2/S_1 crossing are real. This indicates that trajectories released at the crossing with small initial kinetic energy will collect along a valley defined by the MEP corresponding to path **II**. It can be seen from Figure 4a that this MEP involves disrotatory motion of the two terminal methylenes coupled with central C−C bond expansion. At 0.5 au distance there are two low-frequency modes corresponding to disrotatory motion coupled with central C−C bond contraction (78 cm^{-1}) and to conrotatory motion of the two terminal methylenes (178 cm^{-1}). At 1.5 au distance from the S_2/S_1 crossing these frequencies increase to 293 and 354 cm^{-1}, respectively. In the case of compound **1** path **II** (see Figure 4b) is dominated by conrotatory motion of the two terminal methylenes. In the close vicinity of the S_2/S_1 crossing (i.e. at 0.25 au distance) there is a small imaginary frequency (98 i cm^{-1}) which indicates a flat ridgelike shape of the relaxation path. The corresponding vibrational mode describes a distortion dominated by the C−C−C−C torsional coordinate. However, slight progression along the MEP (i.e. at 1.25 au distance from the S_2/S_1 crossing) results in the change of the frequency of this mode to a real 110 cm^{-1} frequency which indicates the presence of a valley-shaped region.

(ii) $S_1 \rightarrow S_0$ Radiationless Decay and photorearrangement. To gain insight in the mechanism of the radiationless deactivation and photoinduced molecular rearrangement in the parent and alkylated dienes we have investigated the structure of their S_1/S_0 crossing region in detail. As discussed above, in *cis*-butadiene, the S_1 relaxation path does not end at a crossing point but reaches a flat region centered on a ***C*$_s$-MIN** stationary point. However, as previously documented,[12a] this point is connected to a fully asymmetric S_1/S_0 conical intersection structure (**S_1/S_0 CI** in Figure 6a) via an almost barrierless path (as reported in Table 1 the transition structure connecting ***C*$_s$-MIN** to the conical intersection disappears at the PT2F level of theory). In Figure 6a we report such path (path **III**) and document the geometrical deformation leading to decay. This deformation (which corresponds to a highly twisted "kink" of the carbon framework) has been recently recognized to be a general feature in the S_1 state of (unsubstituted) short linear polyenes.[22]

The S_0 relaxation occurring just after $S_1 \rightarrow S_0$ decay can also be computationally investigated. In particular, using the IRD method discussed in section 2, it is possible to define and compute (see ref 16b for a previous application) all energy valleys departing from the crossing point and developing along S_0. In Figure 6a we document four different S_1 relaxation paths which originate from the asymmetric **S_1/S_0 CI** structure located for *cis*-butadiene. Path **IV** describes the reactant back formation process (also reported in Figure 3a). Paths **V**−**VII** are photochemical paths since they all describe real (paths **VI**−**VII**) or degenerate (path **V**) reactive processes. In particular, path **V** describes a (single) double-bond isomerization, path **VI** cyclobutene formation, and path **VII** the *stepwise* formation of bicyclobutane via a cyclopropylcarbinyl diradical. A path describing photoinduced *s-cis* to *s-trans* conformational isomerization has not been located.

Comparison of Figure 6a with Figure 6b indicates that decay

(19) Garavelli, M.; Bernardi, F. Olivucci, M.; Vreven, T.; Klein, S.; Celani, P.; Robb, M. A. *Faraday Discussion.* **1998**, *110*, in press.

(20) Miller, W. H.; Handy, N. C.; Adams, J. E. *J. Chem. Phys.* **1980**, *72*, 99−112.

(21) Truhlar, D. G.; Gordon, M. S. *Science* **1990**, *249*, 491−498.

(22) Celani, P.; Garavelli, M.; Ottani, S.; Bernardi, F.; Robb, M. A.; Olivucci, M. *J. Am. Chem. Soc.* **1995**, *117*, 11584−11585.

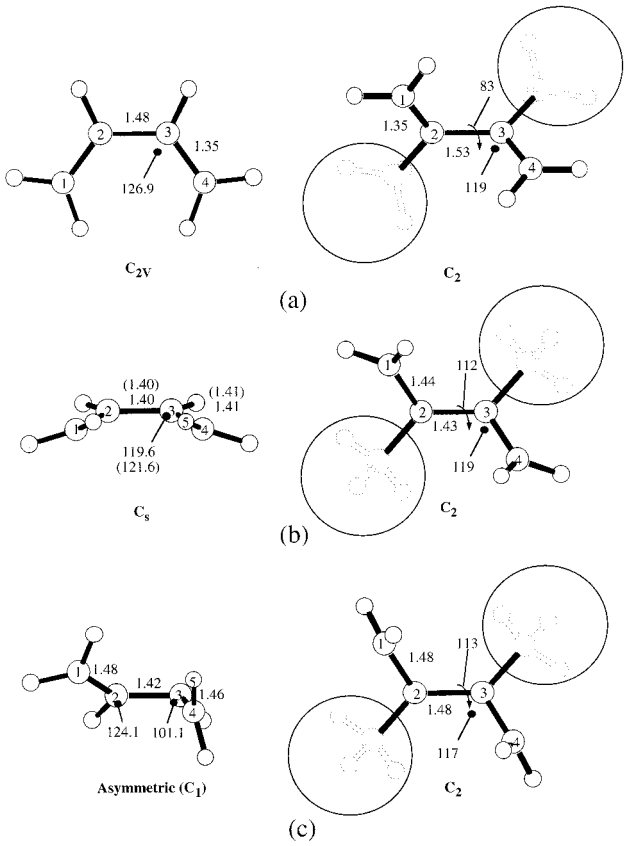

Figure 5. Structure of the computed (a) ground-state reactant, (b) S_2/S_1 intersection point, and (c) S_1/S_0 intersection point for *cis*-butadiene and compound **1** (geometrical parameters in Å and deg).

and photoproduct formation in **1** will be different from that of the parent compound. In fact, as mentioned in the previous subsection, this molecule enters the crossing region directly following S_1 relaxation. Consequently the relevant product formation paths have been determined starting at the **S_1/S_0 CI**. We have located three paths. Path **III** describes the reactant back-formation process (see also Figure 3b), while paths **IV** and **V** describe photochemical processes. Path **IV** is an asymmetric path and, similar to path **V** in the parent compound, describes (single) double-bond isomerization. In contrast path **V** maintains the C_2 symmetry of the reactant and leads to *concerted* bicyclobutane formation. Remarkably, despite several attempts we have not been able to locate a path driving the relaxation toward the monocyclic photoproduct.

The quantum yield of a photoproduct is given by the percent of excited-state molecule that, after decay, relaxes along the valley leading to that photoproduct. The evaluation of this quantity requires, in principle, a dynamic treatment of the nonadiabatic motion on the S_1 and S_0 potential energy surfaces, a challenging problem for a system of the size of compound **1** and even for *cis*-butadiene. Therefore, here, we limit ourselves to a qualitative discussion of the excited-state dynamics and photoproduct formation process. Above we have seen that the structure of the S_2 and S_1 energy surfaces indicates that S_1 decay in *cis*-butadiene is prompted by a motion which has no components along the initial excited-state relaxation (i.e. along path **II**). Thus, intramolecular vibrational relaxation (IVR) from symmetric to nontotally symmetric modes (i.e. path **III**) is required to populate path **III** and initiate $S_1 \rightarrow S_0$ decay. Since during IVR ca. 25 kcal mol^{-1} of vibrational excess energy will be distributed among 24 degrees of freedom, we expect the average velocity along path **III** to be small. Under these

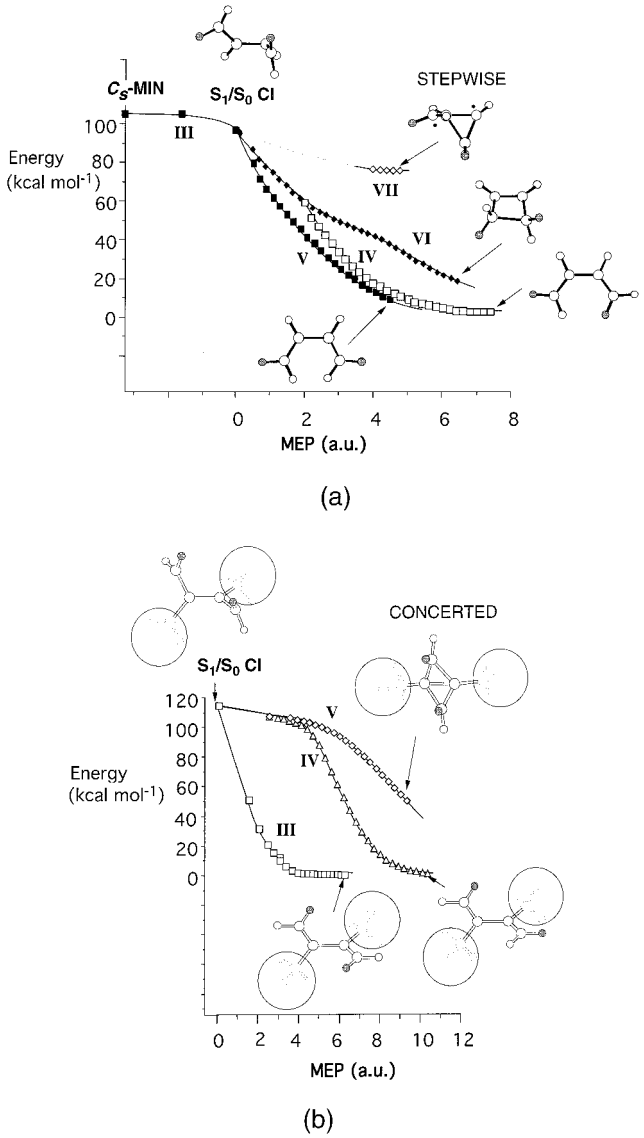

Figure 6. (a) *cis*-Butadiene energy profiles along the five MEPs describing the $S_1 \rightarrow S_0$ decay, S_0 relaxation, and photoproduct formation from ***C_S*-MIN**. The full squares curve on S_1 (2A) defines the *excited state* lowest-lying reaction path (path **III**). The open and full squares curves and the open and full diamonds curves on S_0 define concurrent *ground-state* paths leading to reactant back-formation (path **IV**), double-bond *cis*−*trans* isomerization (path **V**), cyclobutene formation (path **VI**), and bicyclobutane formation (path **VII**), respectively. The energies of all points have been scaled to match the PT2F energies of the ***C_S*-MIN**, ***C_S*/CI-TS**, and **S_1/S_0 CI** points (see Table 1). The structures document the geometrical progression along the relaxation paths. (b) Compound **1** energy profiles along the three MEPs describing the $S_1 \rightarrow S_0$ decay, S_0 relaxation, and photoproduct formation from **S_1/S_0 CI**. The open squares, open triangles, and open diamonds curves define the S_0 concurrent *ground-state* paths leading to reactant back-formation (path **III**), double-bond *cis*−*trans* isomerization (path **IV**), and bicyclobutane formation (path **V**), respectively. The structures document the geometrical progression along the relaxation path.

conditions, the structure of the S_0 potential energy surface in the vicinity of the decay point can provide a qualitative indication of the accessibility of the energy valleys connecting the decay point to the various photoproducts. Several attempts to locate a valley pointing in the direction of path **VII** (i.e. leading to a cyclopropylcarbinyl diradical) in the vicinity of the S_1/S_0 crossing (i.e. the decay channel) have failed. Rather, this valley only starts to exist at a much larger (4.0 au) distance

than the valley defining paths **IV**−**VI**. Thus bicyclobutane formation from *cis*-butadiene is not predicted to be the major photochemical process in this system. In fact, one expects that a system moving in the direction of the tip of the cone will hop to S_0 and populate the, much closer, double bond isomerization and cyclobutene formation valleys. Only a small number of S_1 molecules will have enough kinetic energy to reach the bicyclobutane valley. This seems to be consistent with the undetectable or extremely low[2] production of bicyclobutane from *cis*-butadiene.

The structure of the S_2 and S_1 energy surfaces of compound **1** indicates that, after decay to S_1, the system will relax along a totally symmetric coordinate leading to S_0 "directly". Thus, IVR from totally symmetric modes to other modes is not required to initiate $S_1 \rightarrow S_0$ decay in compound **1**. Furthermore, inspection of the computed S_1 relaxation coordinate indicates that, along this steep path, the molecule accelerates toward a molecular geometry which favors concerted bicyclobutane formation. Indeed, the two terminal methylenes in **1** rotate (see structure evolution in Figure 4b) in such a way to increase the overlap between the sp^2 orbitals on carbons 1 and 3 and carbons 2 and 4 (see also structures in Figure 5b,c). Because of the barrierless nature of path **II** such rotational motion is expected to be impulsively continued after decay to S_0. Notice that this impulsive motion will not favor reactant back-formation because this requires methylene rotation in the opposite direction. Similarly, impulsive production of cyclobutene requires acceleration along the $C_1-C_2-C_3-C_4$ torsional coordinate. However, this torsional angle is almost constant along path **II**. In conclusion, the structures in Figures 4b and 6b support the idea that bicyclobutane production occurs via a *concerted* and *synchronous* mechanism (i.e. with simultaneous formation of two new σ-bonds) also prompted by the excited-state motion. This view is also supported by the finding that the bicyclobutane valley in compound **1** begins much closer (at ca. 2.5 au) to the computed $S_1 \rightarrow S_0$ decay channels (**S_1/S_0 CI**) than in the parent compound. Thus the only favored photoproducts in this molecule appear to be those corresponding to path **IV** (double bond isomerization) and path **V** (bicyclobutane formation).

4. Conclusion

The results presented above provide a rationalization of the different photoproducts observed after irradiation of *cis*-butadiene and of its highly alkylated derivative **1**. The role of the two bulky substituents in prompting the production of the highly strained hydrocarbon bicylobutane (and in inhibiting production of cyclobut-1-ene) is that of driving the relaxation process along a path which is structurally very different from that of the unsubstituted diene. In particular, as shown in Figure 3b, the transient excited-state species (***C_2*-ION**) generated by irradiation of **1** relaxes along a totally symmetric coordinate which leads to the bicyclobutane **2** or, alternatively, to the more stable original reactant on the S_0 energy surface. However, no path leading to formation of the corresponding cyclobut-1-ene derivative has been located. In contrast, the coordinate describing the excited-state relaxation of the parent compound (see Figure 3a) enters the S_0 energy surface at a fully asymmetric structure (**S_1/S_0 CI**). Analysis of the ground-state relaxation paths (see Figure 6a) indicates, consistently with the experimental observation, that cyclobut-1-ene and not bicyclobutane must be the major strained photoproduct of this reaction.

The detailed analysis of the computed reaction coordinate reveals that formation of **2** occurs via a *concerted* and *synchronous* mechanism characterized by a conrotatory motion

Scheme 2

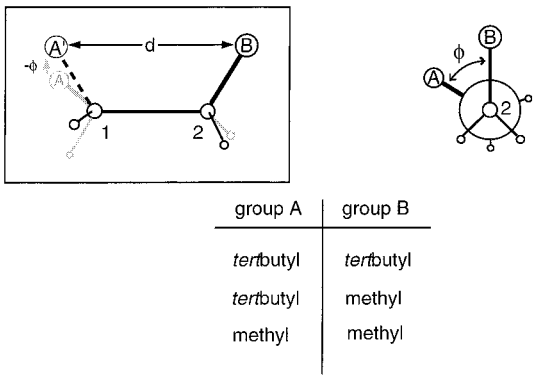

group A	group B
*tert*butyl	*tert*butyl
*tert*butyl	methyl
methyl	methyl

of the two terminal CH_2 of the reactant. This motion sets the orientation of the methylenes in a direction which favors cyclopropane ring closure. Furthermore, the barrierless nature of the S_1 relaxation path in **1** (path **II** in Figure 3b) suggests that formation of the bicyclobutane moiety is facilitated by the impulsive acceleration of the conrotatory methylene rotation along the S_1 energy surface.

Finally, in this paper we have demonstrated that a simple *hybrid* methodology which has been designed to simulate a *tert*-butyl group at the computational cost of a methyl group can be successfully employed in mechanistic studies where bulky (i.e. computationally expensive) substituents are not directly involved in the bond-breaking−bond-forming process. We are now pursuing further applications to larger systems containing more than two bulky substituents.

Acknowledgment. This research has been supported in part by the EPSRC (U.K.) under Grant No. GR/K04811 and by an EU TMR network grant (ERB 4061 PL95 1290, Quantum Chemistry for the Excited State). We are also grateful to NATO for a travel grant (CRG 950748).

Appendix: Parametrization of the *tert*-Butyl−*tert*-Butyl and *tert*-Butyl−Methyl Steric Interactions

The procedure we have followed involves three steps: (a) A two-dimensional cross section of the ab initio RHF/6-31G* energy surface is constructed.. This cross section is defined by scanning the surface along the (ϕ,d) internal coordinates illustrated in Scheme 2.

The coordinate ϕ corresponds to the torsional angle defined by the atoms $C_A-C_1-C_2-C_B$. The coordinate **d** is not a standard internal coordinate. It corresponds to the value of the distance between the "virtual" carbon atom **A′** and carbon **B**. The position **A′** is obtained by rotating the molecule by $-\phi$ (see light arrow in Scheme 2) so that the atoms $C_{A'}$, C_1, C_2, and C_B lie on the *same* plane. In practice one computes the S_0 energy at each point of a grid defined by fixing a value for the ϕ, **d** variables and minimizing the energy respect to the remaining $3n$ - 8 internal coordinates of the molecule (n is the number of degrees of freedom). (b) The $E_{\text{butane}}(\phi,\mathbf{d})$ energy surface computed for *n*-butane is "subtracted" from the energy surfaces computed for 1-*tert*-butylpropane ($E_{tert-\text{butylpropane}}(\phi,\mathbf{d})$) and 1,2-di-*tert*-butylethane ($E_{\text{di}-tert-\text{butylethane}}(\phi,\mathbf{d})$). The ($\phi$,**d**) grids $E_{tert-\text{butylpropane}} - E_{\text{butane}}$ and $E_{\text{di}-tert-\text{butylethane}} - E_{\text{butane}}$ define the *tert*-butyl−methyl and *tert*-butyl−*tert*-butyl repulsion energy relative to the repulsion of two methyl groups. (c) The $E_{tert-\text{butylpropane}} - E_{\text{butane}}$ and $E_{\text{di}-tert-\text{butylethane}} - E_{\text{butane}}$ are parametrized using the following functional form:

$$E(\phi,d) = \frac{V_1(d)}{2}(1 + \cos\phi) + \frac{V_2(d)}{2}(1 - \cos 2\phi) + \frac{V_3(d)}{2}(1 + \cos 3\phi) + V_4(d) \quad (1)$$

where

$$V_1(d) = A_1d^2 + B_1d + C_1$$

$$V_2(d) = A_2d^2 + B_2d + C_2$$

$$V_3(d) = A_3d^2 + B_3d + C_3$$

$$V_4(d) = A_4d^2 + B_4d + C_4 \quad (2)$$

The functional form (1) is derived from the standard MM torsional potential[10] where V_1, V_2, and V_3 are force field parameters. In eq 1 these constants have been replaced by the quadratic functions given in (2). The $V_i(d)$ functions are used to couple the torsional potential with the distance d. Notice that this coupling introduces a dependence of the torsional potential on the values of the bond lengths C_A-C_1, C_1-C_2, and C_2-C_B and of the bending angles $C_A-C_1-C_2$ and $C_1-C_2-C_B$.

In conclusion, two sets of parameters (A_1, ..., A_4, B_1, ..., B_4, C_1, ..., C_4) are derived by fitting the computed $E_{tert-\text{butylpropane}} - E_{\text{butane}}$ and $E_{\text{di}-tert-\text{butylethane}} - E_{\text{butane}}$ surfaces, respectively. The ability of the functional form (1) to reproduce the shape of the ab initio cross sections described above is documented by the resulting 0.0004 and 0.0008 kcal mol^{-1} mean deviation for the *tert*-butyl−methyl and *tert*-butyl−*tert*-butyl data, respectively. Thus, the first set of parameters provides an analytical representation of the *tert*-butyl−methylene repulsions in compound **1** (relative to a methyl−methylene repulsion of **1′**). Notice that this interaction is described by using the *tert*-butyl−methyl repulsive potential parametrized above. In fact, we assume here that the *tert*-butyl−methylene steric interaction is similar to a *tert*-butyl−methyl steric interaction (this assumption has been dictated by the desire to use closed-shell systems for the parametrization). This should be true when the distances between the two groups are sufficiently large as it is for the range of geometries treated in the rest of the paper. The second set of parameters provides an analytical formula for evaluating the *tert*-butyl−*tert*-butyl repulsion in compound **1** (relative to a methyl−methyl repulsion of **1′**).

By differentiating eq 1, one gets an analytical expression which provides the values of the gradients of the two types of interaction. The expressions for the energy (eq 1) and gradient have been implemented in the *Gaussian94* package.[8b] Thus, according to Scheme 1, the ab initio MCSCF energy and gradient of the methyl-substituted system **1′** are changed by adding the three contributions coming from the parametrization of the *tert*-butyl−*tert*-butyl and *tert*-butyl−methylene interactions.

JA982864E